Wave Functions and g-factor of Holes in Ge/Si Quantum Dots

A.V. Nenashev, A.V. Dvurechenskii and A.F. Zinovieva
Institute of Semiconductor Physics,
Siberian Branch of the Russian Academy of Sciences,
630090 Novosibirsk, Russia

(Dated: February 28, 2003)

We investigate theoretically the Zeeman effect on the hole states in quantum dots. In frame of tight-binding approach we propose a method of calculating the g-factor for localized states. The principal values of the g-factor for the ground hole state in the self-assembled Ge/Si quantum dot are calculated. We find the strong g-factor anisotropy – the components g_{xx}, g_{yy} are one order smaller, than the g_{zz}-component, $g_{zz} = 12.28$, $g_{xx} = 0.69$, $g_{yy} = 1.59$. The efficiency of the developed method is demonstrated by calculating of the size-dependence of g-factor and by establishment of the connection with $2D$ case. The g-factor anisotropy increases with the size of the quantum dot. The analysis of the wave function structure shows that the g-factor and its size-dependence are mainly controlled by the contribution of the state with $J_z = \pm\frac{3}{2}$, where J_z is the angular momentum projection on the growth direction of the quantum dot.

PACS numbers: 71.70.Ej, 71.70Fk, 73.21.-b

I. INTRODUCTION

The functionality of modern semiconductor devices relies on the control of electronic charge. However, the carriers do not only carry charge, but also spin. Spin transport has one major advantage compared to charge transport: quantum coherence can be maintained on much larger time scales. Several device applications, such as spin transistors, spin memory, and also the spin quantum computer have been proposed to utilize spin dependent effects in semiconductors. Semiconductor quantum dots (QD), in which carriers occupy discrete energy states, show various spin-related phenomena, including spin degeneracy, exchange interaction, spin blockade, and Kondo physics (for review see Refs.[1–5]). Various promising schemes exploiting the spin of carriers in QD have been proposed recently[6–8].

For successive manipulation of spin in QD it is necessary to know such fundamental spin properties as the effective g-factor, which defines the Zeeman splitting, and the spin relaxation time. On the one hand these magnitudes characterize the material properties of the physical object, on the other hand they characterize the individual electron state. The effective g-factor is directly connected with structure of the wave function of the localized carrier in QD. Here we demonstrate this connection by considering the hole localized state in the self-assembled Si/Ge quantum dot. From fundamental point of view this system attracts much interest, because here both effects of strong quantum confinement and strains define the energy spectrum and they are responsible for the modification of the g-factor.

In bulk semiconductors the motion of electrons and holes in the presence of the spin-orbit interaction gives rise to the g- factor, which is significantly modified compared to the free particle g-factor ($g \approx 2$). As one advances from bulk semiconductors to low-dimensional structures, quantum confinement effects come into play that leads to further strong modification of the g-factor. For electrons this results in the enhancement[9] and high anisotropy of the Zeeman splitting[10]. A comprehensive theory based on the **kp** method was developed to predict a behavior of the electron g-factor in low-dimensional systems including quantum wells[11], wires and dots[12]. Some theoretical results were published for the hole g-factor in quantum wells[13–15]. Recently the attempt to calculate the hole g-factor in quantum dots was taken[16]. To the best of the author's knowledge, there is no detailed theory of the Zeeman effect for holes confined in quantum dots.

Let us start with qualitative analysis of the principal distinctions between two-dimensional ($2D$) case of quantum wells and zero-dimensional ($0D$) case of quantum dots, which are responsible for the g-factor renormalization. A very wide quantum well can be considered as a bulk semiconductor. When the interaction with magnetic field is small in comparison to the quantization energies (or strain-induced splittings in the case of strained semiconductors), the explicit form of the 8×8 **kp** Hamiltonian allows one to obtain immediately the g-factor components for the hole subbands: for heavy hole $g_{\parallel} = 6k$, $g_{\perp} = 0$, for light hole $g_{\parallel} = 2k$, $g_{\perp} = 4k$, where $g_{\parallel}$, $g_{\perp}$ are the components of the effective g-factor tensor for magnetic field parallel and perpendicular to the growth axis z of quantum well respectively; k is the Luttinger parameter (here the small valence-band parameter q is neglected). For narrower quantum wells the uncertainty in component of quasi-impulse k_z increases that leads to the modification of the light hole g-factor owing to the mixing with the split-off valence band states and with the conduction band states[17]. The Lande factor of heavy hole remains unchanged, because the heavy hole states don't mix with the nearest subband states. In the case of ultranarrow quantum wells the hole g-factor is defined by the parameters of the barrier layer.

In the case of quantum dots a new modification of the hole g-factor occurs owing to the spatial confinement not only in the growth direction z, but also in lateral directions x, y. This leads to the uncertainty in k_x, k_y, and as result, to the strong mixing between the light and heavy hole states[17]. The light and heavy hole mixing is left out of account in the theoretical consideration of 2D system, because the states at the bottom of the subband ($k_x, k_y = 0$) are considered usually. In the self-assembled quantum dots formed on the base of strained heterostructures the significant change of the hole g-factor is caused by the inhomogeneity of strains in QD. If one compares the quantum well and the quantum dot, both with growth direction [100], then one finds in the dot nonzero strains ε_{xy}, ε_{xz}, ε_{yz}, which lead to the mixing between the light and heavy hole states. In quantum well these strains are absent. So, in the case of quantum dots the spatial confinement in all three dimensions and the strain inhomogeneity induce the mixing between electronic bands and as result lead to a new modification of the hole g-factor.

Here we have developed a method of calculating the hole g-factor in quantum dots, using the tight-binding approach. This method allows to calculate the g-factor in quantum dots with different shape and different confinement potential. It is applicable down to size of wave function comparable with interatomic distance. This method can be applied also to the electron states in quantum dots.

This paper is organized as follows. In Sec. II we present the general approach for calculation of the g-factor of carriers in QD. In Sec. III we propose an estimation of the g-factor for holes localized in Ge/Si quantum dots and make comparison with results of numerical calculations. Then we calculate the size dependence of g-factor and establish the relationship between the contribution of the state with $J_z = \pm\frac{3}{2}$ and the g-factor value. The probabilities of Zeeman transitions for different directions of external magnetic field are investigated. In Sec. IV we explain obtained results by means of the simplified model of noninteracting subbands.

II. GENERAL APPROACH

The application of magnetic field $\mathbf{H}$ produces the Zeeman interaction energy of the particle, having effective magnetic moment $\mathbf{M}$, which can be written as: $\hat{H} = -\hat{\mathbf{M}} \cdot \mathbf{H}$. The magnetic moment is connected with the angular momentum $\mathbf{J}$ in following way: $\mathbf{M} = g_0\mu_B\mathbf{J}$, where μ_B is the Bohr magneton, g_0 is the Lande factor, which equal to 2 for the particle with only spin magnetism and to 1 for the particle with only orbital magnetism.

Let us introduce the magnetic moment of a hole $\mathbf{M}_{QD}$, measured in unit of the Bohr magneton.

$$\mathbf{M}_{QD} = \mathbf{L} + 2\mathbf{S},$$

where $\mathbf{L}$ is the orbital angular momentum, $\mathbf{S}$ is the spin of the particle. If one needs to calculate g-factor of confined electron in QD, one can use the same expression for magnetic moment differing only in sign. The Zeeman Hamiltonian for localized carrier in the quantum dot is written as:

$$\hat{H}_{QD}(\mathbf{H}) = -\mu_B \mathbf{H}\hat{\mathbf{M}}_{QD} = -\mu_B(\hat{\mathbf{L}} + 2\hat{\mathbf{S}})\mathbf{H}.$$

Even in quantum dots grown along high-symmetry direction [001] the symmetry is not higher than C_{2v}, because of the nonequivalence of directions [110] and [$\bar{1}$10]. Hence the energy levels are twofold degenerate in the absence of magnetic field, and its sublevels constitute the Kramers doublet. For the pair of Kramers-conjugate states the Zeeman contribution to the effective Hamiltonian is written as:

$$\frac{1}{2}\mu_B \hat{\sigma}_i g_{ij} H_j,$$

where $\hat{\sigma}_i$ $(i = x, y, z)$ are the Pauli matrices, and for low-symmetry systems the real tensor g_{ij} is characterized by nine linearly independent components[18]. For a hole (or an electron) in the quantum dot with symmetry not lower C_{2v}, one can choose the system of coordinates (x, y, z), where g_{ij} is characterized by three principal values g_{xx}, g_{yy}, g_{zz}.

When the Zeeman interaction is small in comparison to the confinement energy, the g-factor depends only on the magnetic field direction and can be evaluated by means of the first-order perturbation theory:

$$|g| = 2\sqrt{\langle\psi|\mathbf{n}\hat{\mathbf{M}}_{QD}|\psi\rangle^2 + |\langle\psi|\mathbf{n}\hat{\mathbf{M}}_{QD}|\psi^*\rangle|^2}, \qquad (1)$$

where ψ, ψ^* – are the Kramers-conjugate states, $\mathbf{n}$ is the unit vector in the magnetic field direction. Thus, to calculate matrix elements of the operator $\hat{\mathbf{M}}_{QD}$, one has to determine the wave functions ψ, ψ^* for the hole (or electron) state in the quantum dot. We assume, that the magnetic field does not change significantly the wave function of hole in QD, and use for calculation of matrix elements the eigenstates of the non-perturbed Hamiltonian. We solved the eigenvalue problem for the hole states in QD recently[16]. We used sp^3 tight-binding (TB) approach, including interactions between nearest neighbours only[19,20]. The set of atomic orbital $\{s,\ p_x,\ p_y,\ p_z\}$ for each atom was taken, and state vector length was equal to (number of atoms)×(number of orbitals per atom). Following Chadi[21] the spin-orbit interaction was added to the Hamiltonian. Strain effects[22] were incorporated into Hamiltonian in two ways: as changes of interatomic matrix elements[20,23] and as the strain-induced mixing of orbitals centered on the one atom[16]. In order to find the wave function we applied the free relaxation technique[24]. The component of calculated state vector $\psi_{\alpha N}$ represents the amplitude of the probability to find hole (or electron) on the α-orbital of the atom number N, where the index α runs over the set $\{s, p_x, p_y, p_z\}$.

Since the state vectors were found as linear combinations of atomic orbitals, one should determine the expression for $\hat{\mathbf{M}}_{QD}$ in the representation of atomic orbitals. The angular momentum of electron on the α-orbital of the atom number N can be written as:

$$\hat{L}_i = \frac{1}{\hbar} e_{ijk} \hat{p}_j \hat{r}_k,$$

where e_{ijk} is the unit antisymmetric tensor; indices i, j, k run over the set $\{x, y, z\}$. The momentum operator $\hat{\mathbf{p}} = m\dot{\hat{\mathbf{r}}}$ can be expressed via the coordinate operator $\hat{\mathbf{r}}$ as:

$$\hat{\mathbf{p}} = \frac{im}{\hbar}(\hat{H}_0 \hat{\mathbf{r}} - \hat{\mathbf{r}} \hat{H}_0),$$

where m is the mass of the free electron, $\hat{H}_0$ is the Hamiltonian without spin-orbit interaction. This equation can be deduced from the time differentiation rules for operators[25]. Then the angular momentum operator can be written as:

$$\hat{L}_i = \frac{im}{\hbar^2} e_{ijk} \hat{r}_j \hat{H}_0 \hat{r}_k.$$

Hence the magnetic momentum of hole on the α-orbital:

$$(\hat{M}_{QD})_i = \hat{L}_i + 2\hat{S}_i.$$

But one can not use this equation directly for calculation of the matrix elements $\langle\psi|\hat{\mathbf{M}}_{QD}|\psi\rangle, \langle\psi|\hat{\mathbf{M}}_{QD}|\psi^*\rangle$, because the state vectors ψ, ψ^* are calculated in TB approach and the coordinate operator $\hat{\mathbf{r}}$ has no physical sense in this approach. We replace it by coordinate operator $\hat{\mathbf{R}}$ of the atom with considered orbital:

$$\hat{L}_i = \frac{im}{\hbar^2} e_{ijk} \hat{R}_j \hat{H}_0 \hat{R}_k. \tag{2}$$

By replacing $\hat{\mathbf{r}} \longrightarrow \hat{\mathbf{R}}$, we lose some part of the angular momentum. The remaining part (Eq. (2)) is connected with the envelope function. It is the orbital momentum caused by localization of the carrier in the quantum dot. To obtain the total magnetic momentum $\mathbf{M}_{QD}$ one should take into account the internal orbital momentum corresponding to the atomic orbital. Also one should remember about renormalization of $g_0 = 2$ caused by the interaction of electronic bands.

The hole state in the quantum dot is built mainly from states of the valence band, namely heavy hole band (HH), the light hole band (LH). But the nearest electronic bands also make contribution to the state in quantum dot. The split-off valence band (SO) and the conduction band (CB) are important for the correct magnetic momentum calculation for hole (or electron) state in QD. TB approach, which we used for the solving eigenvalue problem, takes into account not only the interaction of the electronic bands near band gap, but also include the interaction of the HH states with the higher conduction bands. As we will show further the contribution of the remote bands in the hole state in QD are negligible. The wave function of hole (or electron) can be presented in the form:

$$\begin{aligned} |\psi\rangle \;=\; & A_{CB}(\mathbf{R})|CB\rangle + A_{HH}(\mathbf{R})|HH\rangle \\ & + A_{LH}(\mathbf{R})|LH\rangle + A_{SO}(\mathbf{R})|SO\rangle, \end{aligned}$$

where $|CB\rangle$, ..., $|SO\rangle$ are the Bloch functions, and coefficients A_{CB}, ..., A_{SO} can be considered as envelopes and reflect the contributions of the corresponding bands in the state in QD. Every component of the wave function has intrinsic effective spin and interacts with the magnetic field according to Eqs. (3) – (6) in the following paragraphs.

For the degenerate valence band states (Γ_8 band) the Zeeman interaction can be written in the form:

$$\hat{H}(\mathbf{H}) = 2\mu_B(k(\hat{\mathbf{J}}\mathbf{H}) + q(\hat{J}_x^3 H_x + \hat{J}_y^3 H_y + \hat{J}_z^3 H_z)), \tag{3}$$

where $\mathbf{J}$ is the hole effective angular momentum ($J = \frac{3}{2}$), k and q are Luttinger parameters. This equation automatically takes into account the internal orbital momentum corresponded to the atomic orbital.

The strains and confinement effects in the quantum dot lead to the lifting of the valence band degeneracy.

It is convenient for states in the HH band to use an effective HH spin or pseudospin S_{hh} =1/2 to describe its sublevels: as in Ref.[14] we identify $J_z = -\frac{3}{2}$ with $(S_{hh})_z = -\frac{1}{2}$ and $J_z = \frac{3}{2}$ with $(S_{hh})_z = +\frac{1}{2}$. In terms of the pseudospin $\mathbf{S}_{hh}$, the Zeeman Hamiltonian is written as:

$$\hat{H}(\mathbf{H}) = \mu_B g_{hh}(\hat{\mathbf{S}}_{hh}\mathbf{H}). \tag{3a}$$

The same one can make for states in the LH band: $J_z = -\frac{1}{2}$ is identified with $(S_{lh})_z = -\frac{1}{2}$ and $J_z = +\frac{1}{2}$ is identified with $(S_{lh})_z = +\frac{1}{2}$. The Zeeman interaction in the LH band:

$$\hat{H}(\mathbf{H}) = \mu_B g_{lh}(\hat{\mathbf{S}}_{lh}\mathbf{H}). \tag{4}$$

From comparison (3) and (3a) one can conclude that for the heavy hole state, which have $J = \frac{3}{2}$, $J_z = \pm\frac{3}{2}$, the Lande g-factor is $g_{hh} \sim 6k$ (the term with small parameter q can be neglected). The equation (3) we will use in the following.

For the CB and SO states the Zeeman interaction can be written in terms of the effective spin: $\mathbf{S}_c$, $\mathbf{S}_{so}$. For states in the conduction band:

$$\hat{H}(\mathbf{H}) = \mu_B g_c(\hat{\mathbf{S}}_c\mathbf{H}), \tag{5}$$

for states in the split-off band:

$$\hat{H}(\mathbf{H}) = \mu_B g_{so}(\hat{\mathbf{S}}_{so}\mathbf{H}), \tag{6}$$

where g_c is the g-factor of an electron in the conduction band, g_{so} is the g-factor of a hole in the split-off band, and operators $\hat{\mathbf{S}}_c$, $\hat{\mathbf{S}}_{so}$ can be expressed via the Pauli matrices $\hat{\sigma}_x, \hat{\sigma}_y, \hat{\sigma}_z$, $\hat{S}_i = \frac{1}{2}\hat{\sigma}_i$.

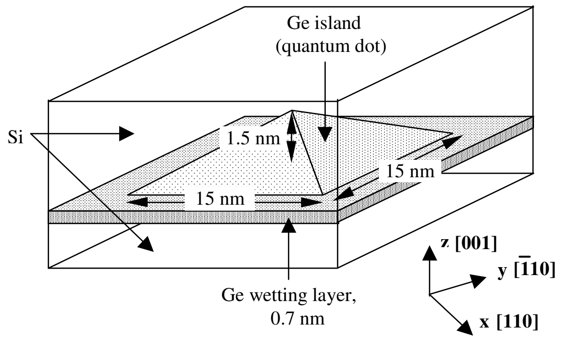

FIG. 1: Geometry of typical Ge/Si(100) quantum dot.

TABLE I: Results of wave function expansion in the basis $|J, J_z\rangle$ for two Zeeman sublevels $|\uparrow\rangle$, $|\downarrow\rangle$ of the ground hole state in Ge quantum dot. The sizes of Ge nanocluster: the height $h = 1.5$ nm, the length of the base side $l = 15$ nm. The contribution of CB states ($\sim 0.5\%$) is omitted.

$\lvert J, J_z\rangle$	$\lvert\frac{3}{2},\frac{3}{2}\rangle$	$\lvert\frac{3}{2},\frac{1}{2}\rangle$	$\lvert\frac{3}{2},-\frac{1}{2}\rangle$	$\lvert\frac{3}{2},-\frac{3}{2}\rangle$	$\lvert\frac{1}{2},\frac{1}{2}\rangle$	$\lvert\frac{1}{2},-\frac{1}{2}\rangle$
$\lvert\uparrow\rangle$	83.67%	2.26%	4.7%	0.08%	1.17%	8.11%
$\lvert\downarrow\rangle$	0.08%	4.7%	2.26%	83.67%	8.12%	0.67%

The total energy of the interaction with magnetic field including the interaction of the orbital momentum $\mathbf{L}$ is written as the sum:

$$\hat{H}(\mathbf{H}) = 2\mu_B(k(\hat{\mathbf{J}}\mathbf{H}) + q(\hat{J}_x^3 H_x + \hat{J}_y^3 H_y + \hat{J}_z^3 H_z)) + \mu_B g_{so}(\hat{\mathbf{S}}_{so}\mathbf{H}) + \mu_B g_c(\hat{\mathbf{S}}_c\mathbf{H}) + \mu_B\hat{\mathbf{L}}\mathbf{H}, \quad (7)$$

where $\hat{\mathbf{L}}$ is given by (2). From this equation one can extract the magnetic moment $\mathbf{M}_{QD}$:

$$(\hat{M}_{QD})_i = 2k\hat{J}_i + 2q\hat{J}_i^3 + g_{so}(\hat{S}_{so})_i + g_c(\hat{S}_c)_i + \hat{L}_i. \quad (8)$$

Substituting Eq. (2) into Eq. (8) we finally arrive at the following main equation:

$$(\hat{M}_{QD})_i = 2k\hat{J}_i + 2q\hat{J}_i^3 + g_{so}(\hat{S}_{so})_i + g_c(\hat{S}_c)_i + \frac{im}{\hbar^2} e_{ijk}\hat{R}_j\hat{H}_0\hat{R}_k. \quad (9)$$

Now we can calculate the g-factor of a hole (or an electron) in the quantum dot utilizing equations (1), (9).

III. RESULTS

A. Hole g-factor in Ge/Si quantum dots

The Ge quantum dots are usually fabricated in Ge/Si heteroepitaxial system (lattice mismatch $\sim$ 4%) by Stransky-Krastanov growth mode after deposition of a few monolayers. The average size of Ge quantum dots in well-known experiments are $\sim 10-20$ nm in lateral direction and $\sim 1-2$ nm in height, and these quantum dots can be viewed as artificial atoms[26]. The large ($\sim$ 0.7 eV) valence-band offset characteristic of Ge/Si heterojunction leads to an effective confinement of holes in Ge clusters[26]. The experimental results show that the shape of Ge/Si quantum dot is close to the square pyramid with the height h one order smaller than the length of the base side l ($h/l \sim 1/10$)[27]. The Ge nanocluster represents quasi-two-dimensional object with the principal symmetry axis z, see Fig. 1.

The localized states in the quantum dot are formed mainly from valence band states, and represent the superpositions of states $|\frac{3}{2},\pm\frac{3}{2}\rangle, |\frac{3}{2},\pm\frac{1}{2}\rangle, |\frac{1}{2},\pm\frac{1}{2}\rangle$ (the states $|J, J_z\rangle$ are the eigenstates of effective angular momentum J and its projection J_z). The states $|\frac{3}{2},\pm\frac{3}{2}\rangle$ can be considered as heavy hole states, $|\frac{3}{2},\pm\frac{1}{2}\rangle$ can be considered as light hole states, $|\frac{1}{2},\pm\frac{1}{2}\rangle$ can be considered as split-off hole states. The strain distribution in quantum dot in general consists of the compression in the plane of the pyramid base and the extension in the growth direction z. In the bulk uniaxially extended semiconductor strains lift the degeneracy of the valence band, making the heavy hole band the highest valence band[28]. For this reason the contribution of the heavy hole states in the ground state in QD must be predominant. The same conclusion follows from estimation of the quantization energies for heavy and light hole. Heavy hole has the much bigger effective mass and the lower quantization energy (compared to those for light hole).

Let us consider the external magnetic field applied parallel to the growth direction, $\mathbf{H} \parallel z$. The interaction energy is determined by the projection of the magnetic momentum on the external field direction, i.e. on the z-direction. Therefore for calculation of the hole g-factor one needs to evaluate the matrix elements of operators: $\hat{J}_z$, $\hat{J}_z^3$, $(\hat{S}_{so})_z$, $(\hat{S}_c)_z$, $\hat{L}_z$.

At first we demonstrate that one can estimate the hole g-factor based only on the results of the wave function expansion in the basis $|J, J_z\rangle$, i.e. the expansion $|\psi\rangle = \Sigma_n A_n(\mathbf{R})|n\rangle$ where n runs over the set $\{|\frac{3}{2},\pm\frac{3}{2}\rangle, |\frac{3}{2},\pm\frac{1}{2}\rangle, |\frac{1}{2},\pm\frac{1}{2}\rangle\}$ (the heavy hole states, the light hole states and the split-off hole states). The contribution of CB states is omitted, because of its small value ($\sim$ 0.5%) according to our calculations. The results of the wave function expansion for the ground hole state in the quantum dot with size $l = 15$ nm, $h = 1.5$ nm are presented in Table I. The contribution of the states with $J_z = \pm\frac{3}{2}$ (the heavy hole states) is about $\sim$ 84% of the ground state. The rest part belong to the states with $J_z = \pm\frac{1}{2}$ (the light and split-off hole states). From the Table 1 one can see, that the state $|\uparrow\rangle$ is formed in general by the states with $J_z = +\frac{3}{2}$ and $J_z = -\frac{1}{2}$, and the state $|\downarrow\rangle$ consists of the states with $J_z = -\frac{3}{2}$ and $J_z = +\frac{1}{2}$.The angular momentum projection of heavy hole part is antiparallel to that of light and split-off hole part. This can be explained by symmetry considerations. The combination of the states with $J_z = +\frac{3}{2}$ and $J_z = -\frac{1}{2}$ remains the same under symmetry transformation of group C_{2v} (π-rotation). The part with $J_z = \pm\frac{1}{2}$ reflects the contributions of the states $|\frac{3}{2}, \pm\frac{1}{2}\rangle$, $|\frac{1}{2}, \pm\frac{1}{2}\rangle$, either of the two is about $\sim 8\%$ of the ground hole state. That is the LH and SO states make the equal contributions to the ground hole state.

If the ground hole state in the quantum dot was formed by the heavy hole states only, the spin up state $|\uparrow\rangle$ would correspond to $J_z = +\frac{3}{2}$, and the spin down state $|\downarrow\rangle$ would correspond to $J_z = -\frac{3}{2}$. The Zeeman splitting in the magnetic field $\mathbf{H} \parallel z$ would be defined as:

$$\begin{aligned} E(H_z) &= 2\mu_B \langle (M_{QD})_z \rangle H_z \\ &= 2\mu_B H_z \left(2k \cdot \frac{3}{2} + 2q \cdot \frac{27}{8} + \langle L_z \rangle \right), \end{aligned} \quad (10)$$

where $\langle (M_{QD})_z \rangle$, $\langle L_z \rangle$ are average z-components of the magnetic and orbital momentum in the state $|\uparrow\rangle$. For estimation the term with small parameter q is neglected in the equation (10), $|q| = 0.06$ (Ref.[29]). If one takes into account the admixture of the light and split-off hole states with $J_z = \pm\frac{1}{2}$, the equation (10) turns into following:

$$\begin{aligned} E(H_z) &= 2\mu_B H_z 2k(a^2 - d^2) \cdot \frac{3}{2} \\ &+ 2\mu_B H_z (2k(b^2 - c^2) + g_{so}(e^2 - f^2)) \cdot \frac{1}{2} \\ &+ 2\mu_B H_z \langle L_z \rangle, \end{aligned}$$

where coefficients a^2, b^2, c^2, d^2 are probabilities of finding in the state $|\uparrow\rangle$ hole with $J = \frac{3}{2}$ and $J_z = \frac{3}{2}$, $J_z = \frac{1}{2}$, $J_z = -\frac{1}{2}$, $J_z = -\frac{3}{2}$ correspondingly. The coefficients e^2, f^2 are probabilities of finding hole with $J = \frac{1}{2}$ and $J_z = \frac{1}{2}$, $J_z = -\frac{1}{2}$ correspondingly. They all are connected with coefficients $A_i(\mathbf{R})$, $i \in \{HH\uparrow, HH\downarrow, LH\uparrow, LH\downarrow, SO\uparrow, SO\downarrow\}$ in following way:

$$a^2 = \int A^2_{HH\uparrow}(\mathbf{R}) d\mathbf{R}, \quad b^2 = \int A^2_{LH\uparrow}(\mathbf{R}) d\mathbf{R},$$

$$c^2 = \int A^2_{LH\downarrow}(\mathbf{R}) d\mathbf{R}, \quad d^2 = \int A^2_{HH\downarrow}(\mathbf{R}) d\mathbf{R},$$

$$e^2 = \int A^2_{SO\uparrow}(\mathbf{R}) d\mathbf{R}, \quad e^2 = \int A^2_{SO\downarrow}(\mathbf{R}) d\mathbf{R}$$

For quantum dots with size $l = 15$ nm, $h = 1.5$ nm, these probabilities are: $a^2 \approx 0.84$, $b^2 \approx 0.02$, $c^2 \approx 0.05$, $d^2 \approx 0$, $e^2 \approx 0.01$, $f^2 \approx 0.08$.

If one excludes the term with $\langle L_z \rangle$, the estimation of the hole g-factor can be done by means following equation:

$$g_{zz} \approx 6k(a^2 - d^2) + 2k(b^2 - c^2) + g_{so}(e^2 - f^2). \quad (11)$$

The valence-band parameters for bulk Ge and Si are well known. The Luttinger parameter k is known from high precision experiments (Ref.[29]) $k = -3.41 \pm 0.03$, but the magnitude of g_{so} is known with poor accuracy, $g_{so} = -10 \pm 3$ (Ref.[30]). However the g-factor is crucially depended on the magnitude of k and weakly depended on g_{so}, and this fact does not lead to the significant error in calculations. More significant correction of g-factor can be expected from difference of parameter k in the strained Ge from its value in unstrained Ge. Experimental values for the Luttinger parameters of strained Ge do not exist in the literature. Therefore we have used a nonlinear interpolation scheme[31] along the concepts of Lawaetz[32], which exactly reproduces the experimental values of the Luttinger parameters of both Si and Ge. Parameter k is mainly depended from $\mathbf{k} \cdot \mathbf{p}$ couplings of the topmost valence band with the s and p antibonding conduction-band states with energy gap E_0 and E'_0, respectively. This allows to express the k in the following form:

$$k = \frac{1}{6}\frac{E_p}{E_0} - \frac{1}{6}\frac{E'_p}{E'_0} + \overline{k}, \quad (12)$$

where

$$E_p = 2/m |\langle X|P_x|\Gamma'_2\rangle|^2,$$

$$E'_p = 2/m |\langle X|P_y|\Gamma'_{15}\rangle|^2$$

are the principal interband momentum matrix elements, $|X\rangle$ is the yz-type wave function of the Γ'_{25} valence-band states in the case where spin-orbit coupling is neglected, $\overline{k}$ is expressed by two constants (G and H_2 in Ref.[32]). The estimation of fundamental gap E_0 in strained Ge follow Van de Walle[28] gives $E_0 \simeq 1.2$ eV. This value is close to E_0 obtained for pseudomorfic Ge film by theoretical study of strained $Si_{1-x}Ge_x$ alloys, coherently grown on a Si(001)[33].

The gap E'_0 in strained Ge can be found follow Lawaetz by scaling E'_0 for initial Ge according to

$$E'_0(s) = E'_0(i)[a(s)/a(i)]^{-1.92},$$

where $a(s)$, $a(i)$ are the lattice constants for strained and unstrained Ge. The momentum matrix elements are inversely proportional to the lattice constant. Hence $E_p(s)$ and $E'_p(s)$ are obtained by scaling their values for unstrained Ge with

$$\delta(s) = \{1 + 1.23[D(s) - 1]\} \left[\frac{a(i)}{a(s)}\right]^2,$$

where $D(s)$ the factor introduced by Van Vechten[34] to account for d electron effects. For unstrained Ge $D(i) = 1.25$. To determinate the $D(s)$ for strained Ge we use the method proposed by Van Vechten and obtain the value $D(s) = 1.13$.

Thus, using $E'_0(Ge) = 3.16$ eV, $E_p(Ge) = 26.3$ eV, $E'_p(Si) = 14.4$ eV (Ref.[32]), we have calculated from equation (12) the Luttinger parameter $k = 2.75$.

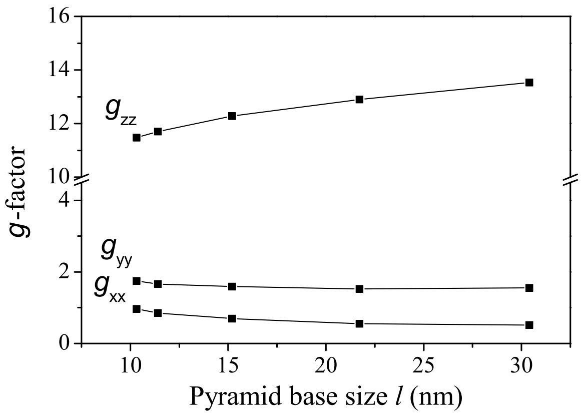

FIG. 2: The g-factor of ground state in Ge quantum dot as a function of the QD lateral size l. The Ge nanocluster height $h = 1.5$ nm.

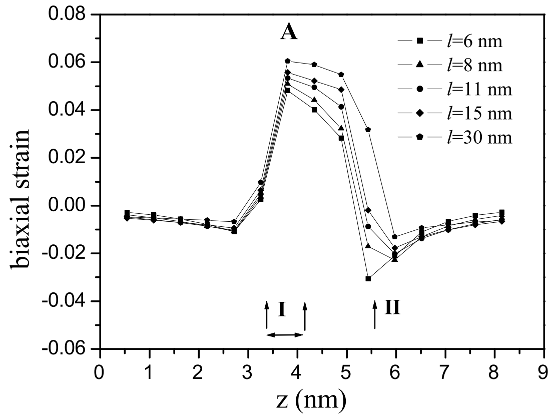

FIG. 3: Profiles of biaxial strain $\varepsilon_{zz} - \frac{1}{2}(\varepsilon_{xx} + \varepsilon_{yy})$ along the symmetry axis z of a quantum dot at different lateral sizes l of Ge nanocluster. The region I corresponds to wetting layer and the point II corresponds to the tip of the pyramid. The maximum value of biaxial strain is reached in wetting layer (point A).

Substituting $k = 2.75$, $g_{so} = 10$ in equation (11), one can find $|g_{zz}| \approx 13$ for Ge nanocluster with $h = 1.5$ nm and $l = 15$ nm . The numerical calculation of the hole g-factor by means Eq.(1) with eigenstates obtained in TB approach gives the value $|g_{zz}| = 12.28$. Analogously we have calculated the principal values of the g-tensor for magnetic field lying in the plane of the pyramid base: $|g_{xx}| = 0.6927$ ($\mathbf{H}$ || [110]), $|g_{yy}| = 1.5907$ ($\mathbf{H}$ || $[\bar{1}10]$).

The comparison of the obtained value g_{zz} with the g-factor of heavy hole in the bulk germanium $|g_{hh}| \approx 6k = 20.46$ shows that the effects of quantum confinement and strains lead to the decrease of the hole g-factor. This demonstrates the suppression of the spin-orbit interaction due to the admixture of the light and split-off holes states.

To estimate the orbital momentum contribution we have calculated the hole g-factor dropped all terms in Eq. (9) except the last. In this case the calculation gives the value of the g-factor one order smaller than for case of total moment $\mathbf{M}_{QD}$: $|g_{zz}| = 0.59$. So, the hole g-factor is mainly determined by the effective angular momentum $\mathbf{J}$, but not by the orbital momentum $\mathbf{L}$.

B. The size dependence of the hole g-factor

The hole g-factor of the ground state in QD demonstrates a well pronounced anisotropy: g_{zz} is one order larger g_{xx}, g_{yy}. Calculation of the hole g-factor for Ge nanocluster with larger lateral size l, keeping the nanocluster height h constant, shows the stronger anisotropy of the g-factor (see Fig. 2). For calculating this size dependence we use the parameter $k = 2.75$ for strained Ge. We do not take into account the change of k with size of Ge nanocluster. Our simple estimation of k in dependence on strain shows that this parameter slightly rise with nanocluster size l. So, if this fact was included into consideration, it would be led to the stronger anisotropy enhancement with lateral size l.

The reason of the g-factor anisotropy lies in the similarity between the ground hole state and the heavy hole state $|\frac{3}{2}, \pm\frac{3}{2}\rangle$, which has the transverse components of the g-factor close to zero[14]. The ground hole state becomes closer to the heavy hole state with increasing of the nanocluster lateral size that leads to the anisotropy enhancement. The numerical calculation confirms this assumption: the contribution of the heavy hole state in the ground state in QD goes up with increasing of the nanocluster size l (see Fig. 2). For example, when the size l changes from 15 nm to 30 nm at the height $h = 1.5$ nm, the contribution of the heavy hole state increases from 83.7% to 86%. The g-factor anisotropy becomes stronger: $|g_{zz}|$ goes up to 13.53, and transverse components decrease to $|g_{xx}| = 0.52$, $|g_{yy}| = 1.56$.

To establish the effects, which govern the change of the contribution of the states with $J_z = \pm\frac{3}{2}$ (the $|\frac{3}{2}\rangle$-states) with nanocluster size l, we consider how the strains in Ge nanocluster are changed. We use our previous results of the calculating the spatial strain distribution in Ge nanocluster and their enviroment[22]. We trace the biaxial stain $\varepsilon_{zz} - \frac{1}{2}(\varepsilon_{xx} + \varepsilon_{yy})$ in dependence on the nanocluster size. When the lateral nanocluster size l increases with $h =$ const, the biaxial strain in the Ge nanocluster increases with the ratio l/h (see Fig. 3). This leads to higher strain splitting between the light and heavy hole states[28]. The admixture of the states with $J_z = \pm\frac{1}{2}$ (the $|\frac{1}{2}\rangle$-states) is decreased. Moreover, our results allow us to comprise the size dependencies of biaxial strain and $|\frac{3}{2}\rangle$-state contribution. It is surprisingly that the dependencies of these characteristics on the nanocluster size l are identical (see Fig. 4). This means that the $|\frac{3}{2}\rangle$-state

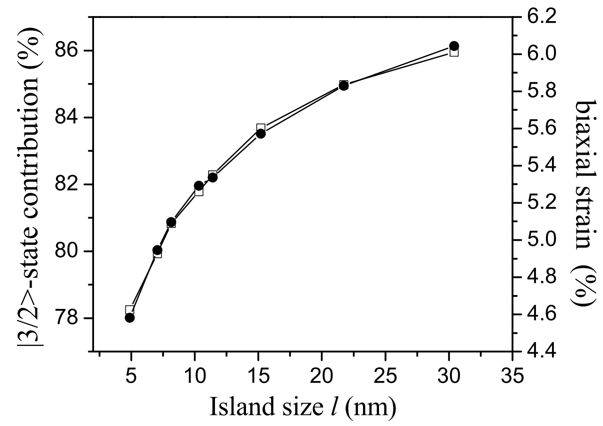

FIG. 4: Size dependence of maximum value of biaxial strain, the height of pyramid $h = 1.5$ nm, the lateral size l is changed. The maximum value of biaxial strain (symbols •) (point A in Fig. 3) depends on the size of Ge nanocluster in the same manner as the $|\frac{3}{2}\rangle$-state contribution (symbols □).

contribution is nearly linear function of biaxial strain. It is difficult to explain this result in frame of simple qualitative model. But it demonstrates that the strain is the main reason determining the change of the contribution ratio between the $|\frac{3}{2}\rangle$-state and the $|\frac{1}{2}\rangle$-state in considered case ($h =$ const, l is changed).

The calculation of the hole g-factor with increasing of both sizes l and h, keeping the proportions of the pyramid constant ($h/l = 1/10$), gives more higher anisotropy of the g-factor. For example, for $l = 30$ nm, $h = 3$ nm the principal values of the g-tensor are following: $|g_{zz}| = 17.43$, $|g_{xx}| = 0.12$, $|g_{yy}| = 1.06$. In this case the contribution of the heavy hole state goes up to 90%, just that leads to this high anisotropy. The strong increasing of g_{zz} is caused by reducing the part of wave function penetrating in Si. In this case the wave function is located almost only in the Ge region, and Si does not affect on the g-factor value. In the case of nanocluster with $h = 1.5$ nm the influence of Si environment is stronger.

When proportions of the pyramid ($h/l = 1/10$) are preserved, strains can not be considered as the main reason determining the $|\frac{3}{2}\rangle$-state contribution. The spatial distribution of strains and their magnitude in the quantum dot are not significantly change with increasing of nanocluster sizes. The strain splitting between the light and heavy hole states remains the same. In Discussion we argue that the reason determining the change of $|\frac{3}{2}\rangle$-state contribution in this case is the confinement energy.

The obtained size dependence of the g-factor proves the correctness of our approach. Indeed, when the lateral size l increases, the Ge nanocluster transforms into the pseudomorphic strained Ge film. The inhomogeneity of the strain distribution disappears, the strains ε_{xy}, ε_{xz}, ε_{yz} are absent. The uncertainty in k_x, k_y becomes equal to zero for the state on the bottom of the subband. All this changes suppress the mixing of the heavy hole state with the nearest band states. And as result, the g-factor of the ground hole state must trend toward the heavy hole g-factor in strained Ge film, $g_{hh} = 6k \approx 16.5$. But for thin Ge layer (thickness is a few nanometers) the g-factor of hole state is affected by Si surrounding Ge, because the tails of wave function penetrate into Si. Namely, for Ge layer with thickness $h = 2.2$ nm the z-component of g-tensor is equal to $g_{zz} = 13.11$. It is obviously, that g_{zz} does not reach the value of heavy hole g-factor in stained germanium. Moreover, this value is smaller than $|g_{zz}| = 13.53$ for Ge nanocluster with $l = 30$nm, $h = 1.5$nm. This effect caused by vanishing the contribution of orbital momentum $\mathbf{L}$ for $2D$ Ge layer.

C. Ge/Si mixing at the interface

The above given values of g-factor have been obtained for Ge nanocluster with atomically sharp Ge/Si interface. We have taken into account the Ge/Si mixing at the interface of real self-assembled quantum dots, and the calculated values have changed. The Ge/Si mixing is introduced in the calculation procedure in the following way: each of atoms in the crystal lattice is substituted with probability $\frac{2}{3}$ for one from its four neighbors. So, in this manner one can obtain the diffused interface with graded changes of the Ge content within three monolayers. The calculation with diffused Ge/Si interface gives the following results: transverse components undergo a drastic change, for example, for the Ge nanocluster with lateral size $l = 15$ nm $|g_{xx}|$ decreases from 0.69 to 0.6, $|g_{yy}|$ decreases from 1.59 to 0.32. But the longitudinal component of the g-factor remains unchanged practically, $|g_{zz}| = 12.37$. So, in the case of diffused interface the g-factor anisotropy enhances in comparison to the case of the atomically sharp interface. Probably, this is caused by the effective increase of the Ge nanocluster size.

D. Zeeman transitions probabilities

For magnetic field $\mathbf{H} \parallel z$, the Zeeman transitions probability depends on the magnitude of the angular momentum projection J_z. For the state with $J_z = \pm\frac{3}{2}$ the transitions between Zeeman sublevels are forbidden, for allowed transitions the condition $\Delta J_z = \pm 1$ must be satisfied. The admixture of the states with $J_z = \pm\frac{1}{2}$ leads to the weakening of this prohibition. Therefore the Zeeman transitions probability becomes higher for nanoclusters with smaller lateral size l. For any chosen direction $\mathbf{h}$ of the magnetic field the Zeeman energy is determined by the projection J_h of the angular momentum on the direction $\mathbf{h}$. When the direction of $\mathbf{h}$ is not parallel with principal axis of symmetry z, the states $|J, J_h\rangle$ can not be considered as the heavy, light and split-off hole states. For example, the state $|\frac{3}{2}, \pm\frac{1}{2}\rangle$ with $J_h = \pm\frac{1}{2}$ can not be considered as the light hole state. The state $|J, J_z\rangle$ is transformed into $|J, J_h\rangle$ in following way:

$$|J, J_h\rangle = \sum_{J_z} R^J_{J_z J_h}(\theta,\varphi)|J, J_z\rangle,$$

where θ, φ are the azimuth and polar angles of the vector $\mathbf{h}$ in the coordinate system (x, y, z), and the matrix R can be expressed via standard rotation matrix: $R^J_{J_z J_h}(\theta,\varphi) = D^J_{J_z J_h}(0, -\theta, -\varphi)$[35].

In the special case $\theta = \pi/2$, $\varphi = 0$ the magnetic field lies in the plane of the nanocluster base and coincides with axis x. Let us consider the heavy hole state with $J_z = \frac{3}{2}$, without any admixture. In the representation $|J, J_z\rangle$ the vector of this state can be written in the following form:

$$|\psi\rangle = a\left|\frac{3}{2},\frac{3}{2}\right\rangle + b\left|\frac{3}{2},\frac{1}{2}\right\rangle + c\left|\frac{3}{2},-\frac{1}{2}\right\rangle + d\left|\frac{3}{2},-\frac{3}{2}\right\rangle = \begin{pmatrix} a \\ b \\ c \\ d \end{pmatrix} = \begin{pmatrix} 1 \\ 0 \\ 0 \\ 0 \end{pmatrix},$$

where squares of coefficients a^2, b^2, c^2, d^2 reflect contributions of the states with corresponding J_z, $a^2 + b^2 + c^2 + d^2 = 1$. Under application of $R^J_{J_z J_h}(\frac{\pi}{2}, 0)$ the heavy hole state transforms into superposition of the states with $J_h = \pm\frac{3}{2}$ and $J_h = \pm\frac{1}{2}$: $\begin{pmatrix} 1 \\ 0 \\ 0 \\ 0 \end{pmatrix} \rightarrow \begin{pmatrix} \sqrt{1/8} \\ \sqrt{3/8} \\ \sqrt{3/8} \\ \sqrt{1/8} \end{pmatrix}$. From this equation it is clear, that the contribution of the state with $J_h = +\frac{1}{2}$ is $\frac{3}{8}$ of whole state, the state with $J_h = -\frac{1}{2}$ makes the same part. They contain together 75%. So, for magnetic field $\mathbf{H}$, lying in the plane of pyramid base, the contribution of the states with $J_h = \pm\frac{1}{2}$ becomes higher in comparison with $\mathbf{H} \parallel z$. Therefore the probability of Zeeman transitions for in-plane magnetic field is higher. This is also true for the hole state with initial admixture of the states with $J_z = \pm\frac{1}{2}$, as for the ground hole state in the considered Ge quantum dot, where the contribution of the states with $J_z = \pm\frac{1}{2}$ is about 16%. Further we present some estimation of Zeeman transitions probabilities for different directions of the magnetic field. The probability of induced transitions between Zeeman sublevels is determined by the interaction of the magnetic momentum with oscillating microwave magnetic field $H_\perp \cos 2\pi\nu t$ ($H_\perp$ is perpendicular to the external magnetic field $\mathbf{H}$) and is proportional to the square of the matrix element $|\langle\downarrow|\hat{\mu}_\perp H_\perp|\uparrow\rangle|$, where $\mu_\perp$ is the magnetic momentum projection on the direction of microwave field $H_\perp$[36],

$$P_{\uparrow\downarrow} \sim |\langle\downarrow|\hat{\mu}_\perp H_\perp|\uparrow\rangle|^2 .$$

For external field $\mathbf{H} \parallel z$ the microwave magnetic field $H_\perp$ lies in the plane of the nanocluster base and the projection of magnetic momentum $\mu_\perp$ is proportional to the principal values of g-tensor: g_{xx} (the direction [110]) and g_{yy} (the direction [$\bar{1}$10]). For microwave field $H_\perp$, which is parallel to the direction [110], the probability is proportional to the square of the principal value g_{xx}: $P_{\uparrow\downarrow} \sim g^2_{xx}$.

For external field $\mathbf{H}\perp z$ the projection of magnetic momentum $\mu_\perp$ lies in the plane containing the axis z. For microwave field $H_\perp$, which is parallel to direction [100], the probability is proportional to the square of the principal value g_{zz}, $P_{\uparrow\downarrow} \sim g^2_{zz}$.

For quantum dot with $g_{zz} = 12.28$, $g_{xx} = 0.69$, $g_{yy} = 1.59$ the estimation of induced transitions probability gives the probability for $\mathbf{H} \parallel z$ approximately two orders smaller than for $\mathbf{H}\perp z$:

$$\frac{P_{\uparrow\downarrow}(\mathbf{H}\perp z)}{P_{\uparrow\downarrow}(\mathbf{H} \parallel z)} \approx 100.$$

If we take into account the decrease of transverse components ($g_{xx} = 0.52$, $g_{yy} = 0.18$), caused by the Ge/Si mixing at the interface, then the ratio amounts to thousand:

$$\frac{P_{\uparrow\downarrow}(\mathbf{H}\perp z)}{P_{\uparrow\downarrow}(\mathbf{H} \parallel z)} \approx 10^3.$$

IV. DISCUSSION

The obtained results give the evidence that the driving force of g-factor size dependence is the change of the contribution of the $|\frac{3}{2}\rangle$-states to the hole state in QD. To explain the existing ratio between contributions of the $|\frac{3}{2}\rangle$-state and the $|\frac{1}{2}\rangle$-state composing the hole state in QD, we apply the simplified model of the band structure without interaction of the electronic bands. We consider separately the energy spectrum of hole with $J_z = \pm\frac{3}{2}$ and the energy spectrum of hole with $J_z = \pm\frac{1}{2}$ in QD (see Fig. 7). In frame of this model the deepest energy levels in QD belong to hole with $J_z = \pm\frac{3}{2}$. In the region of the excited states one can find the levels of both $|\frac{3}{2}\rangle$-states and $|\frac{1}{2}\rangle$-states. If the mixing between the $|\frac{3}{2}\rangle$-states and the $|\frac{1}{2}\rangle$-states is included into consideration then the true spectrum of a hole in QD can be obtained. In the region of the excited states there are some "mixed" states with comparable contributions of both holes. The ground state mainly consists of the $|\frac{3}{2}\rangle$-state. This qualitative model is justified by results of numerical expansion of hole states in QD on the $|\frac{3}{2}\rangle$-states and $|\frac{1}{2}\rangle$-states .

Figure 5 presents the contributions of the $|\frac{3}{2}\rangle$-states for the ground and excited states of confined hole in the quantum dot with sizes $l = 15$ nm, $h = 1.5$ nm. These results show, that the contributions of the $|\frac{3}{2}\rangle$-states are smaller for more excited states than for deeper states. For example, for the first excited state the $|\frac{3}{2}\rangle$-state contribution goes down until 79%, while for the ground state it is about 84%. For the ninth excited state the $|\frac{3}{2}\rangle$-state contribution is about 60% of the wave function.

The contribution of the $|\frac{3}{2}\rangle$-state in the QD hole states is not described by smooth function of the energy. For

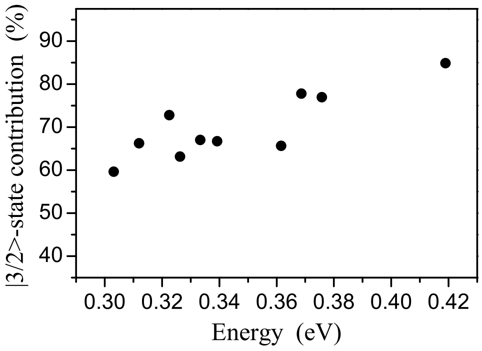

FIG. 5: The $|\frac{3}{2}\rangle$-state contribution for the ground state and nine excited states in Ge quantum dot vs. the state energy. The energy is counted from valence band edge in bulk Si, the energy of the ground state $E_0 = 420$ meV.

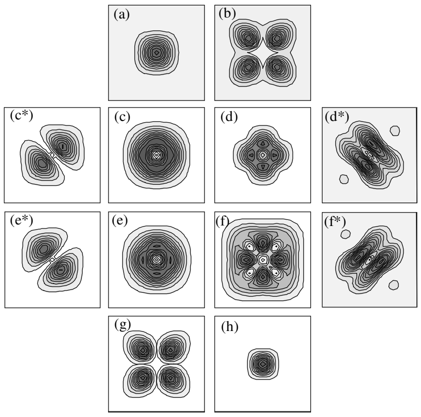

FIG. 6: The wave functions of $|\frac{3}{2}\rangle$-states and $|\frac{1}{2}\rangle$-states for first forth levels in quantum dot: ground state – (a), (b), first excited state – (c), (d), second excited state – (e), (f), third excited state – (g), (h). The center right panel presents $|\frac{1}{2}\rangle$-states, the center left panel - $|\frac{3}{2}\rangle$-states. For clarifying the character of wave functions for first and second excited states we create the superposition of these wave functions $\frac{1}{\sqrt{2}}(|\psi_1\rangle \pm |\psi_2\rangle \cdot \exp(i\varphi))$ with any optimal phase φ, which demonstrates p-like character (see panel with *). The panel (c^*) corresponds to " + ", (e^*) corresponds to " − " in this superposition, both are related to the $|\frac{3}{2}\rangle$-states. Analogously the panels (d^*), (f^*) correspond to the $|\frac{1}{2}\rangle$-states.

explanation of this stepwise change we construct the wave functions of $|\frac{3}{2}\rangle$-states and $|\frac{1}{2}\rangle$-states separately.

The calculated wave functions of these states for the first four levels in QD are presented in Fig. 6. Our results allow to determine the character of wave functions. The $J_z = \pm\frac{3}{2}$ part of the ground state has the s-like wave function. As to part with $J_z = \pm\frac{1}{2}$, which is about 16% of the ground state, it has the d-like wave function. If we consider two spectra of hole with $J_z = \pm\frac{3}{2}$ and with $J_z = \pm\frac{1}{2}$ in our simplified model, then we will find s-like, p-like, d-like, ... states in each spectrum (see Fig. 7). Certainly, the lowest state is the s-like state, then the p-like state follows, the d-like state and so on. A degree of the $|\frac{1}{2}\rangle$-state admixture to the $|\frac{3}{2}\rangle$-state is determined by energy gap between these states and is proportional to $\left(E_{\pm3/2} - E_{\pm1/2}\right)^{-1}$. From the data in Fig. 6 one can conclude that the ground state is formed by mixing of the s-like state from the spectrum of hole with $J_z = \pm\frac{3}{2}$ and the d-like state from spectrum of hole with $J_z = \pm\frac{1}{2}$. In this case the admixture of the $|\frac{1}{2}\rangle$-states is determined by energy gap $\Delta E_0 = E^s_{\pm3/2} - E^d_{\pm1/2}$. The first and the second excited states in QD are formed by mixing of the p-like states from both spectra. At first glance the character of these wave functions is not clear. But its superposition $\frac{1}{\sqrt{2}}(|\psi_1\rangle \pm |\psi_2\rangle \cdot \exp(i\varphi))$ has p-like character (see panels with * in Fig. 6), that allows us to classify its parts as p-like wave functions. In these cases the energy gaps are the same ($\Delta E_1 = \Delta E_2 = E^p_{\pm3/2} - E^p_{\pm1/2}$), and the $|\frac{1}{2}\rangle$-state contributions are equal. The third excited state is formed by mixing the d-like state from the spectrum of hole with $J_z = \pm\frac{3}{2}$ and the s-like state from the spectrum of the hole with $J_z = \pm\frac{1}{2}$. In this case the $|\frac{1}{2}\rangle$-state admixture is determined by energy gap $\Delta E_3 = E^d_{\pm3/2} - E^s_{\pm1/2}$, the distance between the interacting energy levels is smaller and the $|\frac{1}{2}\rangle$-state admixture is higher than for underlying levels. By this way one can find the ratio between the energy gaps in all four cases ($\Delta E_0 > \Delta E_1$, $\Delta E_1 = \Delta E_2$, $\Delta E_2 > \Delta E_3$) and explain the degree of the $|\frac{1}{2}\rangle$-state admixture for the first four levels in the quantum dot. For higher levels the interpretation is more difficult, because the wave functions of these states are more complicate and it is impossible to classify its as s-like, p-like, d-like, ... wave functions. So, the contribution ratio between the $|\frac{3}{2}\rangle$-state and the $|\frac{1}{2}\rangle$-state is determined by the energy gap, which depends on the character of the wave functions of interacting states.

Let us find the reasons determining the change of this ratio with nanocluster sizes h, l. When proportions of the pyramid ($h/l = 1/10$) are preserved, the spatial distribution of strains and its magnitude in the quantum dot are not significantly changed with increasing of nanocluster sizes. The strain splitting between the light and heavy hole states remains the same in this case. The quantum confinement energy becomes smaller for larger nanoclusters, for example, for nanocluster with sizes $l = 100$ nm, $h = 10$ nm it is about a few meV. Therefore the ground hole state shifts to the bottom of the potential well. The excited states are not so sensitive to the change of the quantum confinement energy, because its localization lengths are larger than the nanocluster size. The tails of the wave function penetrate into Si surrounding Ge nanocluster. Hence the shift of the excited states is smaller than for ground state. The energy gap ΔE_0 between the s-like state of hole with $J_z = \pm\frac{3}{2}$ and the d-like state of hole with $J_z = \pm\frac{1}{2}$ increases. Consequently, the $|\frac{1}{2}\rangle$-state contribution to the hole ground state decreases and the wave function becomes closer to the heavy hole state.

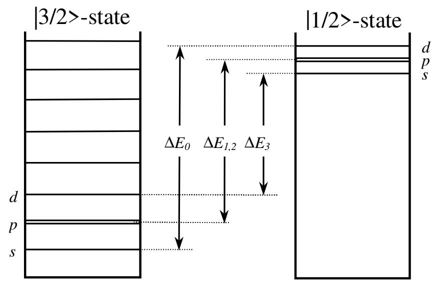

FIG. 7: The schematic sketch of energy spectra of $|\frac{3}{2}\rangle$-states and $|\frac{1}{2}\rangle$-states in the model of noninteracting electronic bands.

In this case the main reason determining the change of the contribution ratio between the $|\frac{3}{2}\rangle$-state and the $|\frac{1}{2}\rangle$-state is the quantum-confinement factor (the change of the confinement energy).

The obtained results give the evidence that the knowledge of the hole wave function structure is very important for interpretation of magnetic properties.

Experimentally the hole g-factor is usually obtained from optical measurements. In these experiments the photoluminescence spectra in magnetic field are studied[37–39]. The g-factor of hole was derived from experimental value of exciton g-factor (g_{ex}) and electron g-factor (g_e), using the equation $g_{ex} = g_h \pm g_e$ ("-" for bright excitons, "+" for dark excitons). To avoid the systematic inaccuracy caused by existing of exchange interaction between electron and hole, one must carry out the experiment with "free" hole (not bounded in exciton). It may be the magneto-tunnelling experiment, which is analogous to experiment with an electron[40]. In this case the choice of the direction of magnetic field plays important role, because the Zeeman splitting and the probability of Zeeman transitions are in strong dependence on the magnetic field direction. For direction $\mathbf{H}||z$ Zeeman transitions are almost forbidden. But in the case $\mathbf{H}\perp z$ the Zeeman splitting is vanished. Therefore it would be better to carry out the experiment in the tilted magnetic field, when the ground hole state in QD is sufficiently splitted and Zeeman transitions are allowed.

V. SUMMARY

We have studied the effect of the external magnetic field on the hole states in the Ge/Si quantum dots. We have developed a method for calculation of the hole (or electron) g-factor in quantum dots, using tight-binding approach. The size dependence of the principal values of the hole g-factor for Ge/Si quantum dot have been calculated.

We have found the significant difference between g-factor of the hole ground state in QD and $g_{hh} = 6k$ (the effective heavy hole g-factor in the strained bulk semiconductor). With increasing of the nanocluster size this difference reduces and the hole g-factor in QD trends toward the heavy hole g-factor. We conclude that the effects of quantum confinement and strains lead to the suppression of the spin-orbit interaction due to the admixture of the light and split-off holes states and the decrease of the effective angular momentum of hole.

We give the recipe of the estimation of the hole g-factor in QD, based on the knowledge of the structure of wave function only. Firstly, one should analyze the wave function, separate the contribution of the main electronic band and calculate the admixture of the nearest bands. Secondly, one should calculate the g-factor of whole state taken into account contributions of all significant bands. Each electronic band has its intrinsic g-factor. The final value of the g-factor of whole state will be the sum of the intrinsic g-factors of each parts with its weighting coefficients. This estimation does not take into account the contribution of the orbital momentum, but in the case of Ge/Si QD this leads to inessential deviation from true value of the g-factor.

The method of the g-factor calculation proposed in this paper allows to carry out the analysis of the existing experimental data and to compare them with theoretical values of the carrier g-factors in quantum dots, grown in different heterostructures, since it can be applied not only to the Ge/Si system.

[1] L. P. Kouwenhoven, C. M. Marcus, P. L. McEuen, S. Tarucha, R. M. Westervelt, and N. S. Wingreen, *in: L. L. Sohn and L. P. Kouwenhoven and G. Schön (Eds.), Mesoscopic Electron Transport, NATO ASI series E 345* (1997), pp. 105–214.
[2] L. P. Kouwenhoven, D. G. Austing, and S. Tarucha, Rep. Progr. Phys. **64**, 701 (2001).
[3] S. Tarucha, D. G. Austing, T. Honda, R. J. van der Hage, and L. P. Kouwenhoven, Phys. Rev. Lett. **77**, 3613 (1996).
[4] L. P. Kouwenhoven, T. H. Oosterkamp, M. W. S. Danoesastro, D. G. A. M. Eto, T. Honda, and S. Tarucha, Science **278**, 1788 (1997).
[5] S. Sasaki, S. D. Franceschi, J. M. Elzerman, W. G. van der Wiel, M. Eto, S. Tarucha, and L. P. Kouwenhoven, Nature **405**, 764 (2000).
[6] D. Loss and D. P. DiVincenzo, Phys. Rev. A **57**, 120 (1998).
[7] G. Burkard and D. Loss, Phys. Rev. B **59**, 2070 (1999).
[8] P. Recher, E. Sukhorukov, and D. Loss, Phys. Rev. Lett. **85**, 1962 (2000).
[9] M. Bayer, V. B. Timofeev, T. Gutbrod, A. Forchel, R. Steffen, and J. Oshinovo, Phys. Rev. B **52**, R11623 (1995).
[10] V. K. Kalevich, B. P. Zakharchenya, and O. M. Fedorova, Fiz. Tverd. Tela **37**, 154 (1995).
[11] E. L. Ivchenko and A. A. Kiselev, Sov. Phys. Semicond. **26**, 827 (1992).
[12] A. A. Kiselev, E. L. Ivchenko, and U. Rössler, Phys. Rev. B **58**, 16353 (1998).
[13] A. A. Kiselev and L. V. Moiseev, Phys. Sol. State **38**, 866 (1996).
[14] X. Marie, T. Amand, P. Le Jeune, M. Paillard, P.Renucci, L. E. Golub, V. D. Dymnikov, and E. L. Ivchenko, Phys. Rev. B **60**, 5811 (1999).
[15] A. A. Kiselev, K. W. Kim, and E. Yablonovitch, Phys. Rev. B **64**, 125303 (2001).
[16] A. V. Dvurechenskii, A. V. Nenashev, and A. I. Yakimov, Nanotechnology **13**, 75 (2002).
[17] G. L. Bir and G. E. Pikus, *Symmetry and Strain-Induced Effects in Semiconductors* (Wiley, New York, 1974).
[18] A. Abragam and B. Bleaney, *Electron Paramagnetic Resonance of Transition Ions* (Clarendon Press, Oxford, 1970).
[19] D. J. Chadi and M. L. Cohen, Phys. Status Solidi (b) **68**, 405 (1975).
[20] J. C. Slater and G. F. Koster, Phys. Rev. **94**, 1498 (1954).
[21] D. J. Chadi, Phys. Rev. B **16**, 790 (1977).
[22] A. Nenashev and A. V. Dvurechenskii, JETP **91**, 497 (2000).
[23] J.-M. Jancu, R. Sholz, F. Beltram, and F. Bassani, Phys. Rev. B **57**, 6493 (1998).
[24] A. A. Kiselev and U. Rössler, Phys. Rev. B **50**, 14283 (1994).
[25] L. D. Landau and E. M. Lifshits, *Quantum Mechanics* (Nauka, Moscow, 1989).
[26] A. V. Dvurechenskii, A. I. Yakimov, V. A. Markov, A. I. Nikiforov, and O. P. Pchelyakov, Izv. Acad. Nauk Fiz. **63**, 307 (1999).
[27] A. I. Yakimov, A. V. Dvurechenskii, Y. Y. Proskuryakov, A. I. Nikiforov, O. P. Pchelyakov, A. S. Teys, and A. K. Gutakovskii, Appl. Phys. Lett. **75**, 1413 (1999).
[28] C. G. Van de Walle, Phys. Rev. B **39**, 1871 (1989).
[29] J. C. Hensel and K. Suzuki, Phys. Rev. Lett. **22**, 838 (1969).
[30] R. L. Aggarwal, Phys. Rev. B **2**, 446 (1970).
[31] R. Winkler, M. Merkler, T. Darnhofer, and U. Rössler, Phys. Rev. B **53**, 10858 (1996).
[32] P. Lawaetz, Phys. Rev. B **4**, 3460 (1971).
[33] G. Theodorou, P. C. Kelires, and C. Tserbak, Phys. Rev. B **50**, 18355 (1994).
[34] J. A. V. Vechten, Phys. Rev. **182**, 891 (1969).
[35] V. F. Gantmakher and Y. B. Levinson, *Carrier Scattering in Metals and Semiconductors* (North Holland, Amsterdam, 1987).
[36] S. A. Altshuler and B. M. Kozyrev, *Electron Paramagnetic Resonance* (Moscow, 1961), p. 20.
[37] M. Bayer, A. Kuther, F. Forchell, A. Gorbunov, V. B. Timofeev, F. Schäfer, J. P. Reithmaier, T. L. Reinecke, and S. N. Walck, Phys. Rev. Lett. **82**, 1748 (1999).
[38] A. Zrenner, M. Markmann, E. Beham, F. Findeis, G. Böhm, and G. Abstreiter, J. of Electronic Materials **28**, 542 (1999).
[39] M. Bayer, O. Stern, A. Kuther, and A. Forchel, Phys. Rev. B **61**, 7273 (2000).
[40] H.-A. Engel and D. Loss, Phys. Rev. Lett. **86**, 4648 (2001).